Influence of NbC Content on the Wear Resistance of Alumina/Niobium Carbide Tools

V. L. Arantes[a] ![ORCID], L. M. Genova[a], P. H. B. P. Guimarães[a], C. A. Fortulan[a] ![ORCID], J. Vleugels[b]

[a]Universidade de São Paulo, Faculdade de Engenharia de São Carlos, Av. Trabalhador São Carlense, 400, São Carlos, SP, Brasil.
[b]KU Leuven, Department of Materials Engineering, Kasteelpark Arenberg 44, B-3001 Heverlee, Belgium.

Wear resistance is a fundamental property which defines the lifetime of cutting tools, but the investigation of wear performance of alternative hard materials for traditional WC-Co composites are recent. The present work evaluated the pin-on-disk wear behavior and mechanical properties, i.e., hardness and fracture toughness of spark plasma sintered Al_2O_3 matrix composites with additions of 5, 15, 25 or 30%wt of niobium carbide NbC. The wear resistance was observed to increase as a function of the NbC content, even though the hardness reached a plateau at 25%wt NbC. The composite behavior was compared to that of other alumina composite tool materials proving to be a promising material for applications such as ceramic cutting tools. The composition A95N5 presented the best combination of values of wear rate: 8.9 mm^3/N.m, hardness equal to (17.36±1.72) GPa and fracture toughness of (3.2±0.6) MPa. $m^{1/2}$.

Keywords: *SPS, cutting tools, ceramic cutting tools, NbC, Al_2O_3.*

1. Introduction

Cutting tools are used in different applications, such as oil and gas winning operations, mining operations and steel and metal machining processes. Among the various cutting tools, we can highlight drill bits, abrasives and cutting inserts.

The most used material for production of cutting tools is Wc-Co. But cobalt and tungsten carbide are linked to a spectrum of risks and health issues. WO_3 and Co_3O_4 have received several notified classifications and labels, in the frame of the European 'Registration, Evaluation, Authorisation and Restriction of Chemical substances programme', also known under the acronym REACH[1]. On the other side, no particular hazards or critical notifications for its oxide (Nb_2O_5) and carbide (NbC) were filed in the framework of REACH. Furthermore, Niobium, on the contrary, is known to be one of the most biocompatible metals.

In particular, cutting tools produced from aluminum oxide (Al_2O_3) present good performance at high cutting speeds when compared to traditional carbide (WC-Co) tools due to the higher hardness and thermal stability, even at high temperatures, due to low thermal conductivity of Al_2O_3, 39 $W.m^{-1}K^{-1}$ when compared to 120 $W.m^{-1}K^{-1}$ of WC. A limiting factor in the use of these materials is their lower fracture toughness (~4,5 $MPa.m^{1/2}$) when compared to hardmetals composed of WC-Co or WC-Ni (11~14 $MPa.m^{1/2}$). In order to improve the performance of Al_2O_3 as material for cutting tools, metal oxides and carbides can be added as tribological reinforcements. Some common reinforcements are zirconium oxide (ZrO_2), titanium carbide (TiC), silicon carbide (SiC) or tungsten carbide (WC) and $MO_2C^{[2-6]}$.

Niobium carbide (NbC) has properties similar to TiC and can be an alternative reinforcement for an Al_2O_3 matrix. In addition, niobium carbide has a high melting point (3610°C) and a hardness (~18 GPa) superior than TiC at high temperatures, between 800 and 1200°C. The combination of hardness and fracture toughness in combination with the fact NbC and Nb_2O_5 are non toxic, offers NbC-Al_2O_3 composites a great potential for application as cutting tools.

In this work, Al_2O_3 matrix composites with niobium carbide additions were investigated. The composites were sintered by spark plasma sintering (SPS), which showed superior results compared to conventional sintering and hot-pressing, owing to fast densification, which is essential for the mechanical properties of these tools[6].

The presence of NbC in the composite acts as a grain growth inhibitor for Al_2O_3, increasing hardness and toughness[7]. However, it complicates the densification of the material, requiring pressure assisted densification. According to previous investigations, a NbC content of 20-30 wt% is necessary to maximize the hardness and wear resistance[8-10].

Dry sliding tribological behavior is a traditional tool for the understanding of tribological behavior of ceramic-based composites, different parameters as tribochemical reactions due surrounding atmosphere or among the tribocouples initiated by frictional heating into the contacting asperities is a key during dry sliding conditions[11]. Typically, the wear of ceramic is characterized by its brittleness behavior, the contact between sphere and disc under load and asperities removal induced by frictional movement. Also, Hertzian stress zone promotes mechanical fracture as radial and median cracks. Initially, ploughing effects are observed, followed by fracture induced third-body abrasion formed by splinters.

Finally, plastic deformation of debris converts them to flakes that are deposited into depressions in the ceramic surface or open cracks forming a tribofilm lubrication, characteristic as adhesive wear[12,13].

The humidity of the surrounding atmosphere presents significant effects on the friction and wear of ceramics. The humidity level of the surroundings promotes surface tribo-reactions as a lubricant film at polycrystalline alumina, increasing the humidity of surrounding air 4% to 10% and the wear rate decreases one order of magnitude and decrease a further order, when relative RH increases from 10% to 50% RH. Above 50%, RH exerts small effect on the amount of wear, although it reaches up levels to saturation, stress concentration comes up and may promote subcritical growth of cracks[13,14].

The improvement of hardness and fracture toughness of the composites reinforced with NbC proves the viability of NbC as an alternative reinforcement for Al_2O_3 matrix tools[8-10]. However, there is a lack of studies assessing the influence of niobium carbide content on the wear behavior of composites Al_2O_3/NbC, an important property concerning the tool lifetime. The present works aims to investigate the influence of the NbC content on the pin-on-disk wear behavior of Al_2O_3/NbC composites against an Al_2O_3 pin.

2. Materials and Methods

2.1. Processing

As raw material, commercial Al_2O_3 (grade A1000SG, Almatis), with >99% purity and an average $d_{50} = 0.45$ µm particle size was used. Niobium carbide was supplied by Treibacher with a purity >99% and $d_{50} = 1.18$ µm.

The composites were produced with variable levels of NbC (5, 15, 25 and 30%wt) in the alumina matrix and will be referred to in the work as A95N5, A85N15, A75N25 and A70N30, respectively. The starting powders were mixed in ethanol for 24 hours in a Turbula multidirectional mixer with a rotation speed of 75 rpm. WC-6%wt Co milling balls were used in a ball to powder weight ratio of 4, in a polypropylene jar. After mixing, the ethanol was removed on a rotative evaporator at 65 ºC, for 2 hours. The dried powders were inserted to a graphite mold and compacted under a pressure of 14 MPa at room temperature.

The pre-compacted samples (at 14MPa) set-ups were Spark Plasma Sintered (HPD-25/1, FCT System GmbH, Germany) in vacuum (4Pa) with a pulse/pause frequency of 10/5 ms and heating rate of 300 ºC/min. The pressure was gradually increased from 2.2 MPa to 30 MPa between 1050 ºC and 1500ºC with 5 min of soaking time. Afterward, the pressure was reduced to 2 MPa, with a cooling rate of 200ºC/min.

2.2. Characterization

The bulk density of the ceramics was measured by the immersion method based on the Archimedes principle, according to standard ASTM C-20[15]. The theoretical density was calculated from the starting powder composition, assuming a density of 3,98 g/cm³ and 7,81 g/cm³ for Al_2O_3 and NbC, respectively.

The microstructure of polished surfaces was examined using optical microscopy. In this process, the polished ceramics were immersed in boiling phosphoric acid for 3 minutes in order to reveal the grain boundary. After 3 minutes, the samples were removed from the acid and immediately immersed in boiling water to interrupt the chemical reaction of the attack without causing thermal stresses that could cause cracks.

Vickers hardness was measured on a Leica Vickers micro durometer model VM HT Leica VNHT MOT with a load of 2 kg. The reported values are the mean and standard deviation of ten indentations. The fracture toughness was calculated by the Antis and Chantikul formula[16], based on the size of the radial crack pattern at the corners of the Vickers indentations. The fracture toughness its calculated according to Equation 1.

$$K_{IC} = 0.016 \left(\frac{E}{H} \right)^{\frac{1}{2}} \left(\frac{P}{c^{\frac{3}{2}}} \right) \qquad (1)$$

where is K_{IC} is the fracture toughness (MPa.m$^{1/2}$), E is the composite Young's modulus, calculated by the mixtures rule (GPa), H is the Vickers hardness of the material (GPa), calculated from the generated impression, P is the applied load (N) and c is the crack length measured from the indentation center. The tests were made on the Vickers hardness instruments present in the Department of Materials Engineering at the School of Engineering of São Carlos, University of São Paulo. The cracks were measured with a Axiotech Zeiss Optical Microscope.

Wear tests were performed following ASTM G99-17[17] on a pin-on-disk machine designed and validated in a recent work[16]. A roughness measurement of the ceramics was made with a Mitutoyo SJ-201P surface roughness tester with 0.25 mm cutoff.

In the test, commercial 6 mm Al_2O_3 spheres (Industrie Bitossi, Italy) were used as pins, because the material has high hardness and chemical inertness. Also, it allows a better comparison with other studies cited here, in which others authors also used alumina pins. The sphere was pressed against the sample surface with a load of 2 kg, at a distance of 2 mm from the center of the rotating sample holder, obtaining a diameter wear track of 4 mm. The sliding speed between the sphere and the sample was 0.1 m/s and the test were performed until a total sliding distance of 500 m was reached, at room temperature and relative humidity equivalent to 50%.

The worn surfaces were measured by a 3D measuring laser microscope, model LEXT-OLS4100 Olympus. In the test, the average of the worn transverse section area of the profiles was determined, which multiplied by the perimeter of the wear track, defined the worn volume of the materials. Six measurements were made for each composite material. The dimensional wear coefficient or the wear rate was calculated by Equation 2.

$$k = \left(\frac{V}{N.m} \right) \qquad (2)$$

where k is the wear rate, V is the worn volume, N the applied load and m is the total sliding distance. For analysis of the

wear mechanisms, Olympus BX60M optical microscopy and FEI Inspect F50 scanning electron microscopy were used.

3. Results and Discussion

The average values obtained for the relative density and roughness of the polished composites are presented in Table 1. All composites showed high density values, which is indicative of the effectiveness of the SPS densification technique. The ceramics showed plane surfaces after polishing, with a roughness below the maximum limit of 0.80 µm. Due to the high content of Al_2O_3, the A95N5 composite was rougher but still within the limits defined by the standard. Polishing of Al_2O_3, is extreme difficult because the grains are easily pulled out of the matrix resulting in a higher roughness. The surface quality, including topography and open porosity has a great influence on the wear rate (18) and will be considered in the evaluation of the results.

Figure 1 presents polished surfaces of the selected compositions observed by optical microscopy. The microstructure is typical for Al_2O_3-NbC[4,5,9,10,18-20], with a gray Al_2O_3 matrix background with white dispersed rounded polygonal NbC particles. The dark regions of composites with addition of 5%

NbC presented a small level of porosity, which corresponds to the black regions in Figure 1a. All composites showed a good dispersion of the NbC particles in the Al_2O_3 matrix, which ensures homogeneous properties.

Figure 2 shows the grain size in function of NbC content. As shown in recent studies, a larger amount of NbC provides smaller Al_2O_3 grain sizes, which is supposed to improve the hardness[9,10,17].

Table 2 presents the hardness results for selected samples. Assuming pure Al_2O_3 and NbC have Vickers hardness of 17.3 and 19.6 GPa[10,18], respectively, the hardness of the composites is predicted to range from 17.4 (5 wt% NbC) to 17,7 (30 wt% NbC) GPa, based on the volumetric mixture rule. The measured hardness clearly increased as a function of the NbC content, but much more proportional than predicted. The increase in the hardness with the addition of a second phase can be explained by the restriction of the plastic deformation of the matrix phase in the neighborhood of the reinforcement particles, changing the crack propagation mechanisms and the type of fracture and also by decreasing the grain size of the matrix[6,18]. As shown in recent studies, a larger amount of NbC provides smaller Al_2O_3 grain sizes, increasing the hardness[9].
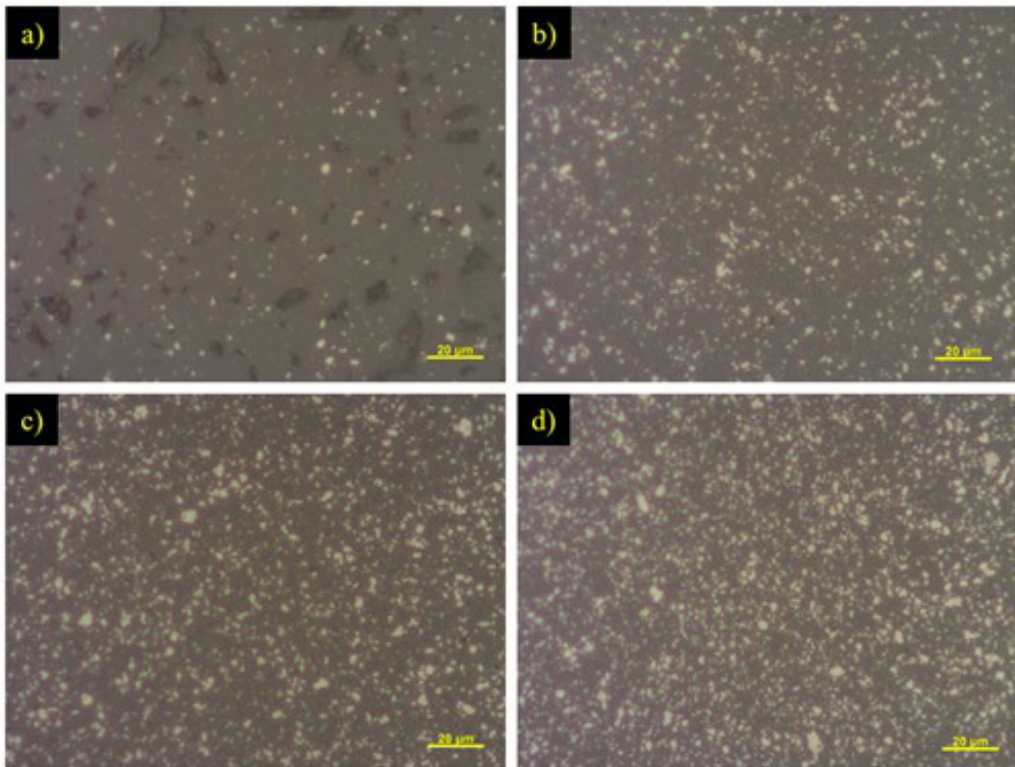
Figure 1. Optical micrographs of polished and etched composite surfaces: a) A95N5, b) A85N15, c) A75N25, d) A70N30.

Table 1. Density and roughness of the ceramic composites

Ceramic	Theoretical density (g.cm⁻³)	Relative Densities (%)	R_a (µm)
A95N5	4.1	98.4	0.57
A85N15	4.3	99.5	0.10
A75N25	4.5	99.9	0.10
A70N30	4.7	99.2	0.10
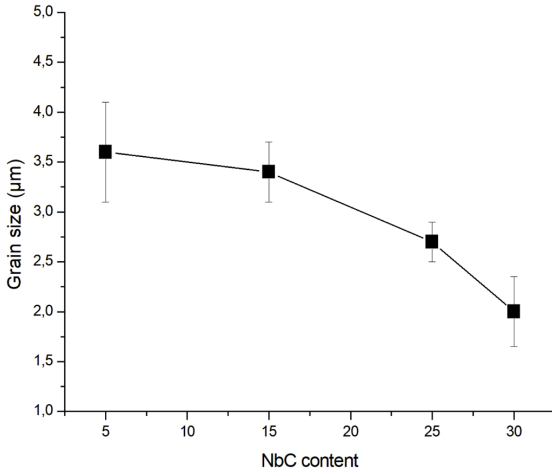
Figure 2. Grain size as a function of NbC content.

Table 2. Hardness of NbC-Al_2O_3 samples for various NbC contents

Ceramic	Predicted hardness (GPa)	Hardness (GPa)
WC-15Co		15,25[21]
A95N5	17.37	17.36 ± 1.72
A85N15	17.60	20.79 ± 1.32
A75N25	17.83	21.48 ± 0.78
A70N30	17.74	21.72 ± 1.22

Although the hardness increases with the increase in NbC content, it reached a plateau value at 25 wt% NbC. In the literature, there is a wide range of reported hardness data for composites owing to differences in the processing routes, responsible for distinct microstructures. Our results are close to the earlier reported values for Al_2O_3-NbC composites, ranging from 15.6 GPa to 26.0 GPa, depending on the processing route and indentation load[9,18-20].

There was no significant variation in the indentation toughness (Table 3) as a function of the NbC content. This corroborates literature values, that presented values between 2.5 and 4.5 MPa.m$^{1/2}$[25] and between 3.2 and 5.4 MPa.m$^{1/2}$[24,6,7]. The reason for the toughness range difference between the literature reports is not clear, but possibly due to the different processing routes, such as different particle size, grain size and interface between the reinforcement particles and the matrix.

Although the fracture toughness of the Al_2O_3-NbC composites are lower than the value observed for WC-Co hardmetals and alumina composites with other reinforcements like ZrO_2-Al_2O_3 (~8 MPa.m$^{1/2}$), the unique characteristics of the Al_2O_3-NbC composites, such as high hardness, good resistance to high temperatures, chemical inertia and good wear resistance are advantages that make it a good material for cutting tool applications such as for the machining of steel and cast iron[6,20].

The wear volume and wear rate of homogeneous composites based on Al_2O_3-NbC are shown in Table 4. The wear rate and volume decreased with increasing NbC addition. The composition A95N5 presented the highest value of wear rate, which corroborates the deleterious influence

Table 3. Indentation toughness of Al_2O_3-NbC composites

Composition	Fracture toughness
	K_{IC} (MPa.m$^{1/2}$)
WC-15Co	9.7[21]
A95N5	3.2 ± 0.6
85N15	2.8 ± 0.1
A75N25	2.7 ± 0.6
A70N30	2.7 ± 0.7

Table 4. Wear volume and wear rate for the Al_2O_3-NbC composites

Composition	Worn volume (mm^3)	Wear rate (mm^3/N.m)
A95N5	$(4.4 ± 0.9)10^{-2}$	8.910^{-6}
A85N15	$(4.7 ± 1.1)10^{-3}$	9.510^{-7}
A75N25	$(8.3 ± 2.4)10^{-4}$	1.710^{-7}
A70N30	$(2.2 ± 2.3)10^{-4}$	4.610^{-8}

of porosity, determined by investigations of Cui et al.[22]. Cui et al. observed that damage of the ceramic tool material grows as material porosity increases from 0.5% to 2.5%, tough variation of material porosity had less effects on the damage within the Al_2O_3-based ceramic tool reinforced by micro (W, Ti)C.

The classical equation 3 proposed for Evans and Wilshaw[23] deals with modeling for the worn volume and shows the importance of both fracture toughness and hardness, with greater influence of (fracture toughness)$^{5/4}$×(hardness)$^{1/2}$. While the hardness and fracture toughness of the Al_2O_3 composites with addition of 25 and 30 wt% NbC did not show a significant difference, the presence of a higher amount of NbC resulted in a wear volume of A70N30, 1 order of magnitude smaller than for A75N25. This not predictable performance shows the relevance of experimental studies for cutting tool applications where ceramic procedural significantly impact on their tribological behavior.

$$V = \alpha \frac{W^{\frac{5}{4}}}{K_{IC}^{\frac{3}{4}} \cdot H^{\frac{1}{2}}} \cdot l \qquad (3)$$

where V is wear volume, α is proportionality constant, W is normal load, K_{IC} is fracture toughness, H is hardness, and l is the sliding distance.

As one can observe in the results, the hardness itself does not allow to predict the wear rate, since the wear resistance is a system property, which can be influenced by separate or combined chemical, mechanical and thermal variables[24]. For this reason, the wear mechanisms of the studied materials are discussed below, in order to drive the selection of the ideal material for distinct applications.

Applying the resolution of eq.3 with the values of H and K_{IC} measured and presented in Tables 2 and 3 respectively, and maintaining the same other values and experimental conditions, observed the same volume worn sequence presented at Table 4, being that the sample A70N30 would have the least wear, since the samples A75N25, A85N15 and A95N5 show 0.6%, 3.3% and 14.1% more worn volume found for the sample A70N30.

Figure 3 shows a 3D profile image of the wear track on A70N30. The blue sectors are indicative of the deeper areas, therefore, more susceptible to wear than the green ones. The red sectors are the ones with the biggest peaks in the surface, which are caused by local plastic deformation, adhesion of worn debris or debris pile-up. It is possible to observe that the deformed areas in the wear track have a typical circular fracture pattern, repeated throughout the trail. According to literature, this pattern is similar to a "Hertzian" fracture pattern[24,25]. Due to the fragility of the material, the applied load of the spherical penetrator causes a cone crack around the area penetrated in the material, namely Hertzian fracture.

In frictional sliding, a tangential force is introduced by distorting the shape of the circular cracks to a straight shape. In this case, the higher the coefficient of friction the greater the fracture distortion. An initial induction period occurs, with several passes without appreciable wear, before the number of microcracks becomes critical and a few fragments separate from the surface[24,25]. Fragments of particles with different sizes, shapes and weights move at different speeds. Due to turbulence and collision, they are transported between surfaces causing impact at different angles, small debris flows and formation of lateral and radial cracks.

In scanning electronic microscopy (SEM) micrographs (Figures 4 and 5), images of wear tracks and enlargements
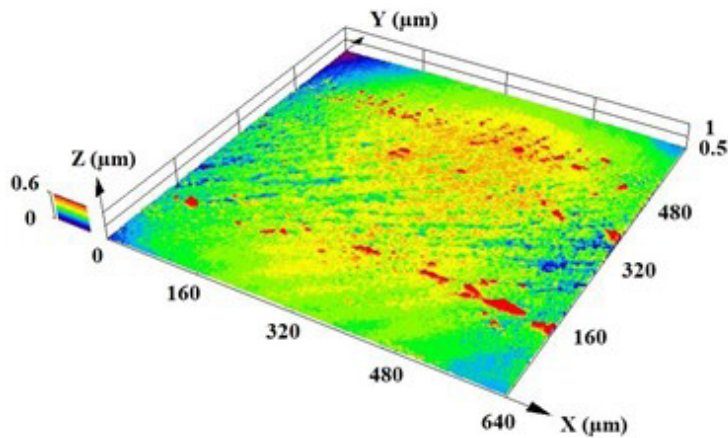
Figure 3. 3D profile of the wear track on the A70N30 composite, where the disc moved in the X direction.
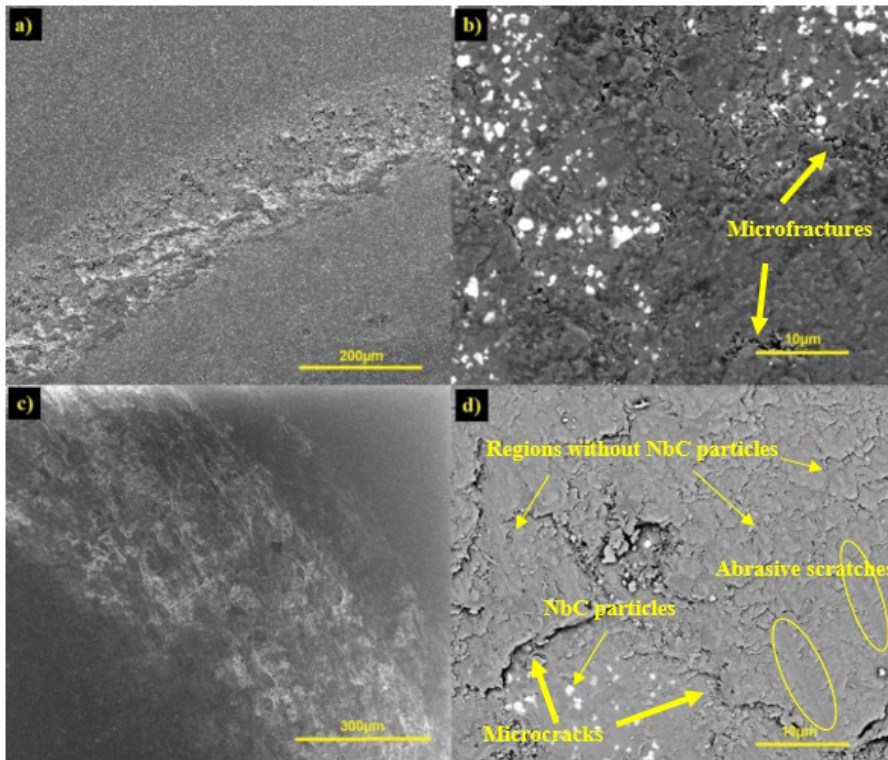
Figure 4. Secondary electrons micrographs of the wear tracks and wear zones of (a,b) A70N30 and (c,d) A75N25.
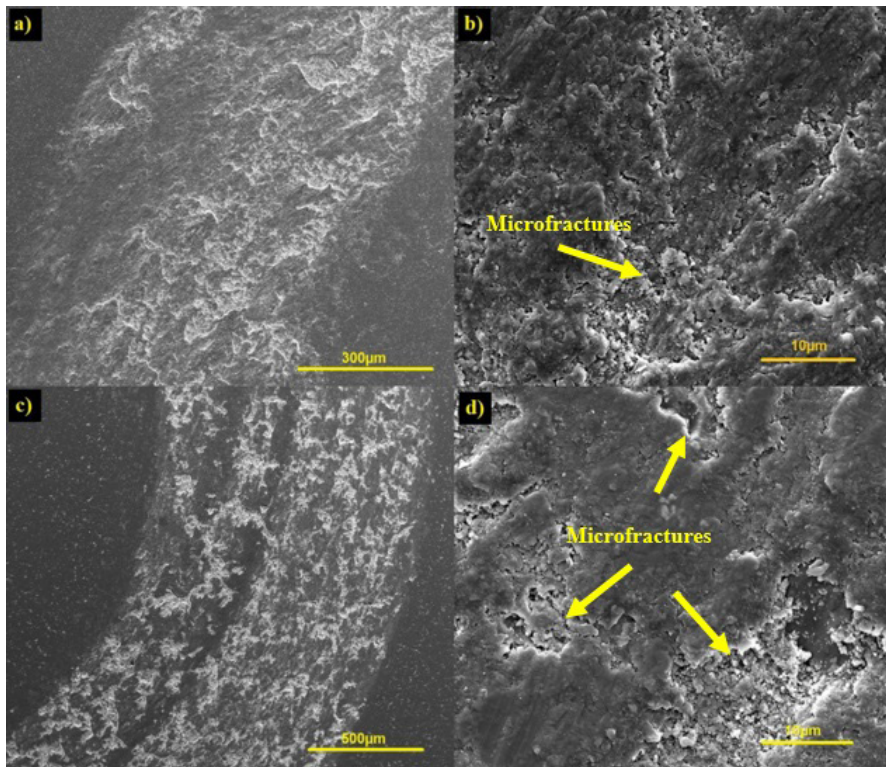
Figure 5. Secondary electron micrographs of the wear tracks and wear zones on A85N15 (a,b) and A95N5 (c,d).

of the worn zone within the track are presented for different Al_2O_3-NbC composites. Microcracks and microfractures caused by cyclic wear stresses are present in all images (see arrows) and the composites with lower NbC content presented a larger quantity and larger dimension of these fractures. This is in accordance with the wear map of Al_2O_3 proposed by Kong and Ashby[25] for pin-on-disk tests, which observed the same dominant mechanisms for Al_2O_3, showing that the addition of NbC can decrease the intensity of these dominant mechanisms. In addition, the widths of the wear trails, that increases with the decrease of NbC content, corroborate the decrease in the volume worn as shown by the results shown in Table 4 and analysis of equation 3.

Some other non-dominant mechanisms occur simultaneously. For example, it is also possible to observe abrasive scratches on A75N25 (circle in Figure 4 (d)). Although, the conditions of the test agree with the wear map proposed by Kong and Ashby[25], wear fragments of particles separated from the surface interact with the pin, generate impacts, adhesions and topographic deformations. This is favorable to other less dominant wear mechanisms, such as abrasive wear.

In Figure 4d, there are regions lacking NbC particles. This suggests that there are adhering films covering regions of the surface. These films can be either alumina hydroxide formed during wear by the reaction of alumina with humidity or material transfer from the pin during the wear process. Ferreira, in his studies of Al_2O_3-NbC composites[18], performed wear tests at different relative humidity levels (from 26% to 76%) and observed that the formation of the films was much more noticeable at higher humidity levels. Tough the tests were carried up at room temperature and a relative

humidity of 50%, the formation of a lubricating Nb_2O_5 tribofilm caused by the oxidation of NbC is also expected, as reported by Woydt and Mohrbacher[4]. These films can promote wear lubrication causing distinct final wear rates.

In figure 6, one can observe the evolution of the coefficient of friction as a function of time during the wear tests. The Al_2O_3 composites with distinct amounts of NbC show similar coefficients of friction, which suggests a similar wear behavior during the tests. In general, for ceramics, the coefficient of friction at the initial running-in-period, increases in a higher rate and thereafter, the frictional behavior is maintained. This can be attributed to the fact that the initial surface asperities of the disc and counterbody get continuously knocked off until the smoothing of the contact surface, given the friction coefficient is related to surface roughness, and higher roughness present lower friction coefficient[26,27]. The different distribution of micro-fractures along the wear track may have caused a change in the sample topography, as well as failures due to surface or subsurface defects, as the re-compaction of debris on the surface, anchored by created defects (cracks and craters) tend to stabilize the wear rate and reduce friction after a long period. An increase in the coefficient of friction can facilitate the wear process due to increasing stresses and heat in the contact area. However, in this case, the highest coefficient of friction of A85N15 had no perceptive influence on the wear rate result when compared to the other composites.

As shown in Figures 4 and 5, alumina can adhere to form peaks that hinder pin movement, increasing the coefficient of friction. When adhesive wear is dominant, the rough peaks present on the surface tend to deform plastically,

increasing the contact area and obstacles that hinder the sliding movement, resulting in a higher coefficient of friction. Therefore, the harder material the lower deformations in the surface and lower the coefficient of friction[28]. A70N30 even
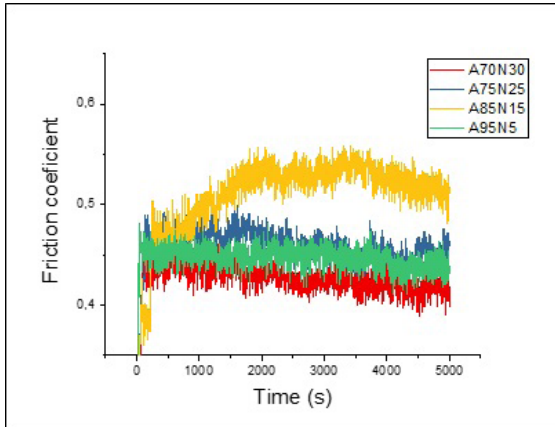
Figure 6. Evolution of the coefficient of friction as a function of time for different Al_2O_3-NbC compositions.
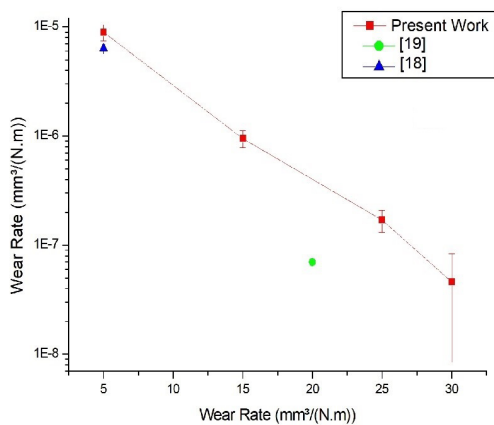
Figure 7. Comparison of the wear rates of Al_2O_3-NbC composites with literature data.
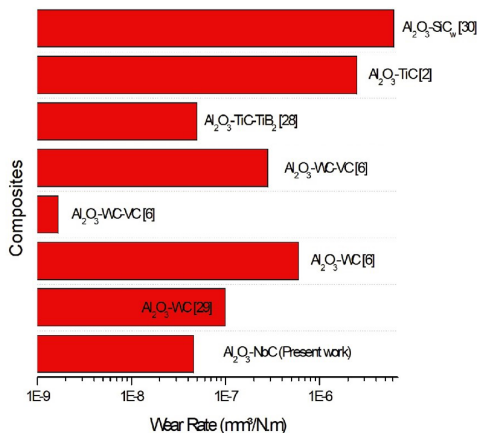
Figure 8. Wear rate of Al_2O_3 composites reinforced with NbC and other reinforcements used in ceramic cutting tools.

shows the lowest coefficient of friction, implying there was no clear correlation between the hardness and the coefficient of friction. This can be influenced by a high resistance to adhesive wear, caused by Nb_2O_3 lubrication effect, which, although not dominant, can occur simultaneously.

Figure 7 presents the wear rates for the different composites, compared to that reported for pin-on-disk tests against Al_2O_3 spheres of Al_2O_3-NbC composites with 20 wt%[19] and 5 wt% of NbC[18]. The wear rate linearly decreased with the NbC content. For additions of 5 wt% of NbC, the literature results[16] were similar to the ones presented in this work. The composition A70N30 showed the best wear behavior.

In wear evaluation, comparison with literature values must be done carefully since wear is a multi-variable system property[28]. Also, there are different techniques of measuring wear rate, as well as distinct accuracies of the equipment. This is even more relevant in materials with a high wear resistance, such as the ones in this study, which suffer microscopic damage that is difficult to detect and to measure precisely.

Figure 8 compares the wear rate of the Al_2O_3-NbC, A70N30 composite, used for Al_2O_3 matrix cutting tools with other reinforcements[2,6,28-30]. It is worth to observe that A70N30 has a relative low wear rate, being among the most wear resistant alumina-based composites and only preceded by Al_2O_3-WC-VC[6] and Al_2O_3-WC[7] composites. The Al_2O_3-WC-VC composite consists of 84 wt% of Al_2O_3, 15 wt% WC and 1 wt% vanadium carbide (VC). The addition of VC as an additive to increase the wear resistance of the composite is essential, since the wear rate rises to about $6.0\ 10^{-7}$ mm^3/N.m for composites with no VC addition.

It is worth to mention that the substitution of WC-Co sphere for a ceramic silicon nitride (Si_3N_4) sphere, promoted the increase of the wear coefficient of Al_2O_3-WC-VC to about $2.8.10^{-7}$ mm^3/N.m^2, which is higher than observed for the Al_2O_3-NbC/Al_2O_3 investigated in the present study ($4.6.10^{-8}$ m^3/N.m). Therefore, it is not possible to compare the performance of different materials precisely if they are not tested under identical conditions. It is difficult to observe literature data for materials subjected to the same wear testing conditions and configurations, due to the complexity and scarcity of tribology work. The comparisons made under the closest conditions indicate that the A70N30 ceramic is among the best non-toxic wear resistant composites reported.

4. Conclusions

The composite obtained by NbC adding in alumina matrix improved wear resistance for inclusions of 5, 15, 25 and 30 wt% and the study adds relevance considerations:

a) The addition of NbC to an Al_2O_3 matrix increases the Vickers hardness, but its benefit tends to reach a limit around 25-30 wt% NbC. There was no correlation between the NbC contents studied and the fracture toughness of the ceramic composites, which was rather constant.

b) Despite the comparable high hardness at 25 and 30 wt% NbC addition, the wear resistance of the 30 wt% NbC composite was substantially higher. This proves that NbC does not improve the wear resistance just by increasing the hardness of the

composite, due to the oxidation of NbC and the formation of a niobium oxide lubricating tribolayer.

c) The wear mechanisms of the Al_2O_3-NbC composites were similar for different NbC contents. The dominant mechanisms was abrasive, but with the recompacting, the behavior became quite characteristic to the adhesive one.

5. Acknowledgments

6. References

1. EC: European Commission. REACH [Internet]. 2020 [cited 2020 Dec 20]. Available from: http://ec.europa.eu/environment/chemicals/reach/reach_intro.htm

2. Yin Z, Yuan J, Huang C, Wang Z, Huang L, Cheng Y. Friction and wear behaviors of Al_2O_3/TiC micro-nano-composite ceramic sliding against metals and hard materials. Ceram Int. 2016;42:1982-9. http://dx.doi.org/10.1016/j.ceramint.2015.10.001.

3. Balbino NAB, Correa EO, Valeriano LC, Amâncio DA. Microstructure and mechanical properties of 90WC-8Ni-2Mo₂C cemented carbide developed by conventional powder metallurgy. Int J Refract Met Hard Mater. 2017;68:49-53. http://dx.doi.org/10.1016/j.ijrmhm.2017.06.009.

4. Woydt M, Mohrbacher H. The use of niobium carbide (NbC) as cutting tools and for wear resistant tribosystems. Int J Refract Met Hard Mater. 2015;49:212-8. http://dx.doi.org/10.1016/j.ijrmhm.2014.07.002.

5. Yin Z, Yuan J, Huang C, Wang Z, Huang L, Cheng Y. Friction and wear behaviors of Al_2O_3/TiC micro-nano-composite ceramic sliding against metals and hard materials. Ceram Int. 2016;42:1982-9. http://dx.doi.org/10.1016/j.ceramint.2015.10.001.

6. Su Q, Zhu S, Ding H, Bai Y, Di P. Effect of the additive VC on tribological properties of WC-Al_2O_3 composites. Int J Refract Met Hard Mater. 2018;75:111-7. http://dx.doi.org/10.1016/j.ijrmhm.2018.04.005.

7. Huang SG, Liu RL, Li L, Van der Biest O, Vleugels J. NbC as grain growth inhibitor and carbide in WC-Co hardmetals. Int J Refract Met Hard Mater. 2008;26:389-95. http://dx.doi.org/10.1016/j.ijrmhm.2007.09.003.

8. Uehara JLHS. Estudo de materiais com gradiente funcional (MGF) a base de alumina (Al_2O_3) e carbeto de nióbio (NbC) obtidos por diferentes técnicas de sinterização [dissertação]. São Carlos: Universidade de São Paulo, 2015.

9. Acchar W, Segadães AM. Properties of sintered alumina reinforced with niobium carbide. Int J Refract Met Hard Mater. 2009;27:427-30. http://dx.doi.org/10.1016/j.ijrmhm.2008.05.004.

10. Pierson H. Handbook of refractory carbides and nitrides: properties characteristics, processing and application. USA: William Andrew Inc., 1996.

11. Magnus C, Kwamman T, Rainforth WM. Dry sliding friction and wear behaviour of TiC-based ceramics and consequent effect of the evolution of grain buckling on wear mechanism. Wear. 2018;422:54-67. http://dx.doi.org/10.1016/j.wear.2019.01.026.

12. Kuzin VV, Fedorov SY, Grigor'ev SN. Tribological aspect in technological assurance of ceramic component quality. Refract Ind Ceram. 2019;60(3):280-3. http://dx.doi.org/10.1007/s11148-019-00353-7.

13. Chen Z, He X, Xiao C, Kim SH. Effect of humidity on friction and wear: a critical review. Lubricants. 2018;6(3):74. http://dx.doi.org/10.3390/lubricants6030074.

14. Perez-Unzueta J, Beynon JH, Gee MG. Effects of surrounding atmosphere on the wear of sintered alumina. Wear. 1991;146(1):179-96. https://doi.org/10.1016/0043-1648(91)90233-K.

15. ASTM International. C20-00: Apparent porosity, water absorption, apparent specific gravity, and bulk density of burned refractory brick and shapes by boiling water. West Conshohocken, USA: ASTM International; 2015.

16. Antis G, Chantikul P. A critical evaluation of indentation techniques for measuring fracture toughness: I, Direct Crack Measurements. J Am Ceram Soc. 1981;64(9):533-8. http://dx.doi.org/10.1111/j.1151-2916.1981.tb10320.x.

17. ASTM International. G99-17: Standard Test Method for Wear Testing with a Pin-on-Disk Apparatus. West Conshohocken, USA: ASTM International; 2017.

18. Ferreira V. Processamento e caracterização mecânica e tribológica do compósito Al_2O_3-NbC [dissertação]. São Paulo: Universidade de São Paulo; 2001.

19. Alecrim LRR, Ferreira JA, Borrell A, Moya M, Pallone EMJA. Análises tribológicas de nanocompósitos de alumina reforçados com carbeto de nióbio e sinterizados por SPS. In: 22° CBECiMat - Congresso Brasileiro de Engenharia e Ciência dos Materiais; 2016; Natal, RN. Proceedings. 2016. Mossoró: UFERSA. p. 2124-35.

20. Alecrim LRR, Ferreira JA, Gutiérrez-González CF, Salvador MD, Borrell A, Pallone EMJA. Sliding wear behavior of Al_2O_3-NbC composites obtained by conventional and nonconventional techniques. Tribol Int. 2017;110:216-21. http://dx.doi.org/10.1016/j.triboint.2017.02.028.

21. Schubert WD, Neumeister H, Kinger G, Lux B. Hardness to toughness relationship of fine-grained WC-Co hardmetals. Int J Refract Metals Hard Mat, 1998;16(2):133-42. https://doi.org/10.1016/S0263-4368(98)00028-6.

22. Cui X, Wang D, Guo J. Effects of material microstructure and surface microscopic geometry on the performance of ceramic cutting tools in intermittent turning. Ceram Int. 2018;44(7):8201-9. https://doi.org/10.1016/j.ceramint.2018.01.269.

23. Evans AE, Wilshaw TR. Quasi-static solid particle damage in brittle solids, I. Observations, analysis and implications. Acta Metall. 1976;24:939-56.

24. Hutchings IM. Tribology: friction and wear of engineering materials. London, UK: Butterworth-Heinema; 1992.

25. Kong H, Ashby MF. Wear mechanisms in brittle solids. Acta Metall Mater. 1992;40:2907-20. http://dx.doi.org/10.1016/0956-7151(92)90455-N.

26. Ravikumar K, Sarkar D, Basu B. ZrO₂-toughened Al_2O_3 composites with better fracture and wear resistance properties. J Biomater Appl. 2018;32(9):1174-86. http://dx.doi.org/10.1177/0885328217750820.

27. Zhang W. A review of tribological properties for boron carbide ceramics. Prog Mater Sci. 2021;116:100718. http://dx.doi.org/10.1016/j.pmatsci.2020.100718.

28. Masanta M, Shariff SM, Choudhury AR. Tribological behavior of TiB₂-TiC-Al_2O_3 composite coating synthesized by combined SHS and laser technology. Surf Coat Tech. 2010;204:2527-38. http://dx.doi.org/10.1016/j.surfcoat.2010.01.027.

29. Su Q, Zhu S, Ding H, Bai Y, Di P. Comparison of the wear behaviors of advanced and conventional cemented tungsten carbides. Int J Refract Met Hard Mater. 2019;79:18-22. http://dx.doi.org/10.1016/j.ijrmhm.2018.10.019.

30. Jianxin D, Zeliang D, Jun Z, Jianfeng L, Tongkun C. Unlubricated friction and wear behaviors of various alumina-based ceramic composites against cemented carbide. Ceram Int. 2006;32:499-507. http://dx.doi.org/10.1016/j.ceramint.2005.03.031.